An Equation of State for Thermodynamic Properties for Methanol

D. Kume[1, 2], N. Sakoda[1] and M. Uematsu[1]

[1] Center for Multiscale Mechanics and Mechanical Systems, Keio University, Hiyoshi 3-14-1, Kohoku-ku, Yokohama 223-8522, Japan.

[2] To whom correspondence should be addressed. E-mail: y09635@educ.cc.keio.ac.jp

• **ABSTRACT**

A new formulation for the thermodynamic properties of methanol in the fluid phase has been developed. This model is a function of reduced temperature and density with 27 terms on the basis of selected measurements of pressure-density-temperature (P, ρ, T), isobaric and isochoric heat-capacity, speed of sound and saturation properties. Based on a comparison with available experimental data, it is recognized that the model represents most of the reliable experimental data accurately in the range of validity covering temperatures from the triple point temperature (175.56 K) to 573 K at pressures up to 200 MPa. The uncertainty in the density calculation is estimated to be 0.5% in the liquid phase and that in the pressure calculation is 0.8% in the vapor phase except in the critical region. The uncertainty of our model are estimated to be 0.2% for vapor pressure, 3% for heat capacities, 1% for the speed of sound in the vapor phase and 3% for the speed of sound in the liquid phase. The behavior of the isobaric heat-capacity, isochoric heat-capacity, speed of sound and Joule-Thomson coefficients calculated by the present model shows physically reasonable. Regarding the behavior of the isobaric and isochoric heat-capacity, graphical comparisons between our model and the IUPAC model are discussed.

KEY WORDS: equation of state; Helmholtz free energy; methanol; thermodynamic properties.

1. INTRODUCTION

In these years, many Asian countries become industrialized and the consumption of energy is increasing in these countries. And Japan needs to improve the self-sufficiency ratio in the energy supply, because she depends extremely on foreign countries for energy sources. She feels also the need of developing alternative fuel. Methanol-Water mixture is expected to be an alternative energy to the oil energy and has attracted great attention due to the easy handling and transport of hydrogen energy. For industrial use, an equation of state (EOS) for the mixture with high accuracy is required. However, we cannot find any equations of state for methanol-water mixtures from the literature retrieval.

The aim of this study is to formulate EOS expressed by the Helmholtz free energy function for methanol-water mixtures. The IAPWS-95 formulation [1] is used widely as the EOS for water. The IUPAC formulation for methanol [2] is popular. We, however, found the serious error in the IUPAC formulation, which is that the behavior of the isobaric specific heat-capacity, C_p, and that of the isochoric specific heat-capacity, C_v, do not show physically reasonable behaviour. Therefore, we have formulated a new equation of state for methanol expressed by the Helmholtz free energy function based on the available experimental data including those reported after the publication of the IUPAC formulation.

2. SELECTION OF INPUT DATA

We compiled about 2100 experimental thermodynamic property measurements for methanol. A summary of data in the single region such as $P\rho T$ data, caloric and acoustic measurements, and saturation property data including saturated vapour pressures, saturated liquid and vapor densities and heat capacity in saturation is listed in Table I. Most of the experimental data reported prior to 1993 were summarized by de Reuck [2] . For our modelling effort, we have converted the temperature values of all experimental data to ITS-90.

The distribution of the single-phase data on a pressure- temperature plane is shown in Fig. 1. In the single-phase region, the $P\rho T$ data of Zubarev [5] , those of Machado [8] , those of Straty [10] , those of Harrison [11] , those of Riembauer [12] and those of Osada

[15] were used as input data. In the liquid region, the $P\rho T$ data of Osada [15] is of the highest priority because the uncertainty of their data is very small (show Table I). In the temperature range above 420 K where the data of Osada [15] do not cover, the data of Machado [8] were used as input data. Regarding the data of Straty [10] , only the data points above the critical temperature were used as input data in the fitting process. Other sets of data were used only for comparison with our model. With respect to caloric and acoustic properties, four sets of experimental measurements, three sets of speed-of-sound, W, data [31-33] and isochoric specific heat-capacity, C_v, data of Kitajima [3], were used as input data. The distribution of saturated vapor pressures is shown in Fig. 2 and that of saturated densities are shown in Fig. 3. The saturated property data used for our modelling are indicated with superscript asterisks in Table I. The data selection wes determined according to the selection of IUPAC model [2] and the selected data were used as input data to provide ancillary correlations discussed in the next section. The saturated-liquid heat capacity data of Carlson [28] were used as additional data in the nonlinear fitting process.

A summary of reported critical parameter values is listed in Table II. For our modelling, the values of the critical temperature, density and pressure determined by IUPAC model are adopted. These values are based on the data reported by Harrison and Gammon [11] with use of law of rectilinear diameters.

3. ANCILLARY CORRELATION

In this study, the following three ancillary correlations for the saturation properties (P_s: saturated vapor pressure in MPa, ρ^{V}: saturated vapour density in kg·m^{-3} and ρ^{L}: saturated liquid density in kg·m^{-3}) were developed on the basis of the selected experimental data indicated by superscript asterisks in the Table I.

$$\ln\frac{P_s}{P_c}=\frac{1}{1-x}\left(A_1x+A_2x^{1.5}+A_3x^{2}+A_4x^{3.5}\right) \tag{1}$$

$$\ln\frac{\rho^{V}}{\rho_c}=B_1x^{0.2}+B_2x^{0.8}+B_3x^{2.5}+B_4x^{4.5}+B_5x^{8.0} \tag{2}$$

$$\ln\frac{\rho^{L}}{\rho_c}=C_1x^{1/6}+C_2x^{0.3}+C_3x+C_4x^{2.4} \tag{3}$$

where P_c is the critical pressure, 8.1035 MPa, $x = 1 - T / T_c$, and ρ_c is the critical density, 275.56 kg m^{-3}. The coefficient in Eqs. (1)-(3) are listed in Table III. The saturated property data calculated by Eqs. (1)-(3) were used as sets of supplementary input data for the present modeling.

These ancillary correlations are not required for calculating saturated properties but provide good estimates when calculating saturated properties iteratively from the present model by the application of the Maxwell criterion.

4. FUNDAMENTAL EQUATION OF STATE

We formulated the dimensionless Helmholtz free-energy model given by Eqs. (4), which consists of the ideal-gas state contribution, $\phi^0(\tau, \delta)$, expressed by Eq. (5), and the residual real state fluid contribution, $\phi^r(\tau, \delta)$, expressed by Eq. (6).

$$\phi(\tau,\delta) = \frac{a}{RT} = \phi^0(\tau,\delta) + \phi^r(\tau,\delta) \tag{4}$$

$$\phi^0(\tau) = f_1 + f_2 \ln\tau + f_3\tau + \sum_{i=4}^{10} f_i \ln\{\exp(g_i\tau) - 1\} \tag{5}$$

$$\phi^r(\tau,\delta) = \sum_{i=1}^{6} n_i \tau^{t_i} \delta^{d_i} + \sum_{i=7}^{15} n_i \tau^{t_i} \delta^{d_i} \exp(-\delta) + \sum_{i=16}^{24} n_i \tau^{t_i} \delta^{d_i} \exp(-\delta^2) + \sum_{i=25}^{26} n_i \tau^{t_i} \delta^{d_i} \exp(-\delta^3) + n_{27} \tau^{t_{27}} \delta^{d_{27}} \exp(-\delta^4) \tag{6}$$

where $\tau = T_c / T$ is the inverse reduced temperature, $\delta = \rho / \rho_c$ is the reduced density and a denotes the Helmholtz free energy in J·kg^{-1}. R is the gas constant for methanol with $R = R_m / M$, where the universal gas constant, R_m = 8.314472 J·mol^{-1}·K^{-1} [40] , and M is the molar mass, 32.04216 kg·mol^{-1} [2] . The coefficients for Eqs. (5) and (6) are listed in Tables IV and V, respectively. The ideal-gas part of the present model Eq. (5) is the same as the IUPAC model [2]. In process of formulating our model, it was found that the data of Ta'ani [7] in the liquid region deviate systematically from those of Machado [8]. Because of this reason and possible decomposition of methanol in the high temperature region [2], we rid

input data of all data of Ta'ani [7]. The specific entropy is given a value of zero at 298.15 K and 0.1 MPa in the ideal gas state and the specific enthalpy is given a value of zero at 298.15 K in the ideal gas state.

5. COMPARISONS WITH EXPERIMENTAL DATA

5.1. $P\rho T$ Property Comparisons

Figure 4 shows pressure deviations of the available $P\rho T$ measurements in the vapor phase from the present model. In this paper, the vapor phase means densities smaller than the critical density, whereas the liquid phase means densities larger than the critical density. The $P\rho T$ data of Petty [4] cover the range of temperatures from 267 to 411 K at pressures from 0.07 to 1.0 MPa. Our model represents these data with pressure deviations from –2.2 to +0.1 %. The data of Zubarev [5] in the vapor phase covering the range of temperatures from 413 to 573 K and of pressures from 0.38 to 16.9 MPa deviate systematically from the present model by –1.9 to +0.6%. Similarly, the data of Harrison [11] in the vapor phase, which covers the range of temperature from 503 to 533 K, represent systematical deviations from our model by –1.8 to 1.0%. The data of Fischer [6] , which are represented with pressure deviations from –0.3 to 1.6%, cover the range of temperatures from 310 to 632 K at pressures from 0.02 to 0.2 MPa. These deviations increase with decreasing temperature. With respect to the data of Bich [9] , the present model is in good agreement with their measurements with pressure deviations from –0.1 to 0.4%.

Figure 5 shows density deviations of the available $P\rho T$ measurements in the liquid phase from the present model. The data of Osada [15] , which is included in input data, are represented within ± 0.16%. The data of Yokoyama [16] and those of Kitajima [3] agree well with our model within ± 0.2%, whereas the data of Machado [8] deviate from our model by –0.3 to +0.5%. The present model represents the data of Harrison [11] with density deviations from –0.5 to +0.8% except for some data points in the region near the critical point. The data of Zubarev [5] and those of Straty [10] in the liquid region deviate from our model by –3.0 to 2.0%. In the low temperature region, the data of Riembauer et al. [12] is reported their data from 183 to 213 K and Vacek and Hany [13] reported their data from 207 to 293 K. The present model represents well the data of Riembauer [12] within

0.21%, whereas those of Vacek [13] from –0.1 to +0.9%. Most of the density values of Vacek are larger than the calculated values.

5.2. Saturation-Property Comparisons

Deviations of thermodynamic properties along the saturation boundary from the present model are shown in Figs. 6-8. Fig 6 shows deviations of the saturated vapor pressure. The present model represents most of the saturated vapor-pressure within ± 0.2 %. Deviations of saturated liquid densities are shown in Fig. 7. The present model represents well the data of Yergovich [24] within ± 0.06% and those of Osada and Yokoyama within ± 0.2%. The calculated values from the ancillary correlation, Eq. (1), for the saturated vapor pressure and those from Eq. (2) for the saturated liquid density agree with our model within ± 0.25% except for the calculated values close to the critical temperature. There are few data for the saturated vapor density of methanol. The available data for the saturated vapor densities deviate from the present model by –0.1 to 4.8%, as shown in Fig. 8.

5.3. Caloric and Acoustic Property Comparisons

Figs. 9-11 show the relative deviations of the experimental measurements of C_p, C_v and W from the present model. Deviations of the available C_v measurements increase with increasing temperature. With respect to C_p, the present model represents the data of Calrson [28] within ± 3% and those of Counsell [29] within ± 2.5%. Two sets of the W data of Sun [30,31] in the liquid phase are represented with deviations from - 4 to 2.7%, whereas the acoustic data of Boyes [32] in the vapor phase are represented from –1 to 0.1%.

6.BEHAVIOR OF DERIVED THERMODYNAMIC PROPERTIES

The behavior of the isobaric specific heat-capacity, C_p, isochoric specific heat-capacity, C_v, speed-of-sound, W, and the Joule-Thomson coefficient, μ, has been calculated with the present model over a temperature range from 176 to 800 K at pressures up to 200 MPa. These results are shown in Figs. 12-15 , respectively. In Figs. 12 and 13, it is clear that the behavior of the C_p and C_v using our model differ from the behavior using the

IUPAC model. However, these four figures based on the present model demonstrate physically reasonable behavior over the entire range of temperatures and pressures.

7.CONCLUSION

We have developed an equation of state for methanol that is valid for temperature from the triple point temperature (175.63 K) to 573 K at pressure up to 200 MPa based on selected experimental data for $P\rho T$, caloric, acoustic and saturation properties. The present model represents accurately experimental thermodynamic property data of methanol in the fluid phase. Behavior of the calculated isobaric and isochoric specific heat-capacities, speed of sound and Joule-Thomson coefficients has been confirmed to be reasonable in the range of validity of our model.

Based on the results of comparisons between the present model and experimental data discussed in the previous chapter, the uncertainty in the density calculation is estimated to be 0.5% in the liquid phase and that in the pressure calculation is 0.8% in the vapor phase except in the critical region. And the uncertainty of our model are estimated to be 0.2% for vapor pressure, 3% for heat capacities, 1% for the speed of sound in the vapor phase and 3% for the speed of sound in the liquid phase.

Finally, as compared to the IUPAC model [2] , the present model corrects serious error in the IUPAC model regarding the behavior of the isobaric and isochoric specific heat-capacities. It also shows thermodynamic consistency in representing the thermodynamic properties over the entire range of temperatures and pressures with a shorter dimensionless Helmholtz free-energy function than the IUPAC formulation.

REFERENCES

1. Release on the IAPWS Formulation 1995 for the Thermodynamic Properties of Ordinary Water Substance for General and Scientific Use, IAPWS(1995)
2. de Reuck,K.M.and Craven,R.J.B.,*Methanol Int. Thermodynamic Table of Fluid State-12*,Blackwell,Oxford,(1993)
3. H. Kitajima, N. Kagawa, S. Tsuruno, H. Endo, Nippon Kikai Gakkai Rombunshu, B-hen. **59**:1921 (2003).
4. L.B. Petty, J.M. Smith, *Ind. Eng. Chem.*, **47**:1258 (1955).
5. V.N. Zubarev, A.V. Bagdonas, *Thermal Eng*., **16**:139 (1969).
6. S. Fischer, H. Köheler, G. Opel, *Wiss. Zeitschr. Univ. Rostock*, **21**:181 (1972).
7. R. Ta'ani, Dr. Ing. Dissertation, University of Karlsruhe (1976).
8. J.R.S. Machado, W.B. Streett, *J. Chem. Eng. Data*, **28**:218-223 (1983).
9. E. Bich, R. Pietsch, G. Opel, *Z. Phys. Chem.(Leipzig)*, **265**:396 (1984).
10. G.C. Straty, A.M.F. Palavra, T.J. Bruno, *Int. J. Thermophys.*, **7**:1077(1986).
11. R.H. Harrison, B.E. Gammon, Private communication to the IUPAC Centre, (1989).
12. M. Riembauer, L. Schulte, A. Würflinger, *Z. Phys. Chem. Neue Folge*, **16**:653 (1990).
13. V. Vacek, A.M. Hany, *Fluid Phase Equilib.*, **76**:187 (1992),
14. C. Xiao, H. Bianchi, P.R. Tremain, *J. Chem. Thermodyn*. **29**:261 (1997).
15. O. Osada, M. Sato, M. Uematsu, *J. Chem. Thermodyn*. **31**:451 (1999).
16. H. Yokoyama, M. Uematsu, *J. Chem. Thermodyn*. **35**:813 (2003).
17. H.F. Gibbard, J.L. Creek, *J. Chem. Eng. Data*, **18**:308 (1974).
18. D. Ambrose, C.H.S. Sprake, R. Townsend, *J. Chem. Thermodyn*., **7**:185 (1975).
19. K. Aim, M. Ciprian, *J. Chem. Eng. Data*, **25**:100 (1980).
20. I. Cervenková, T. Boublik, *J. Chem. Eng. Data*, **29**:425 (1984).
21. A. Zawiswa, *J. Chem. Thermodyn*., **17**:941 (1985).
22. Th.W. de Loos, W. Poot, J. de Swaan Arons, *Fluid Phase Equilib.*, **42**:209 (1988).
23. A.L. Lydersen, V. Tsochev, *Chem. Eng. Technol*., **13**:125 (1990).
24. T.W. Yergovich, G.W. Swift, F. Kurata, *J. Chem. Eng. Data*, **16**:222 (1971).
25. J.L. Hales, J.H. Ellender, *J. Chem. Thermodyn*., **81**:177 (1976).
26. T.F. Sun, J.A. Schouten, N.J. Trappeniers, S.N. Biswas, *J. Chem. Thermodyn*., **20**:1089 (1988).
27. W.B. Kay, W.E. Donham, *Chem. Eng. Sci*., **4**:1 (1955).
28. E. Strömsöe, H.G. Rönne, A.L. Lydersen, *J. Chem. Eng. Data*, **15**:286 (1970).
29. H.G. Carlson, E.F. Westrum, *J. Chem. Thys*., **54**:1464 (1971).
30. J.F. Counsell, D.A. Lee, *J. Chem. Thermodyn*., **5**:583 (1973).
31. T.F. Sun, S.N. Biswas, N.J. Trappeniers, C.A. Seldom, *J. Chem. Eng. Data*, **33**:325 (1988).
32. T.F. Sun, J.A. Schouten, S.N. Biswas, *Ber. Bunsenges. Phys. Chem*., **94**:528 (1990).
33. S.L. Boyes, M.B. Ewing, A.R.H. Goodwin, *J. Chem. Thermodyn*., **24**:1151 (1992).

34. K.A. Kobe, R.E. Lynn, *Chem. Rev.*, **52**:117 (1953).
35. J.M. Skaates, W.B. Kay, *Chem. Eng. Sci.*, **19**:431 (1964).
36. A.P. Kudchadker, G.H. Alani, B.J. Zwolinski, *Chem. Rev.*, **68**:659 (1968).
37. V.N. Zubarev, P.G. Prusakov, L.V. Sergeeva, GSSSD, (1973).
38. R.J.B. Craven, K.M. de Leuck, *Int. J. Thermophys.*, **7**:541 (1986).
39. R.D. Goodwin, *J. Phys. Chem. Ref. Data*, **16**:799 (1987).
40. P.J. Mohr, B.N. Taylor, *J. Phys. Chem. Ref. Data*, **28**:1713 (1999).

FIGURE CAPTIONS

Fig. 1. Distribution of experimental $P\rho T$ data. (▲) Petty [4], (△) Zubarev [5], (◨) Fischer [6], (◇) Ta'ani [7], (+) Machado [8], (◎) Bich [9], (×) Straty [10] , (○) Harrison [11], (◭) Riembauer [12], (●) Vacek [13], (◆) Xiao [14], (◑) Osada [15], (⊕) Yokoyama [16], (□) Kitajima [3].

Fig. 2. Distribution of experimental data for the saturated vapor pressure. (□) Gibbard [17], (▽) Ambrose [18], (◎) Aim [19], (▲) Cervenkova [20], (◇) Zawiswa [21], (×) de Loos [22], (○) Harrison [11], (+) Lydersen [23], (◑) Osada [15], (⊕) Yokoyama [16], (∗) Critical Point.

Fig. 3. Distribution of experimental data for the saturated vapor and liquid density. (+) Yergovich [24], (▲) Hales [25], (◇) Zawiswa [21], (□) Sun [26], (○) Harrison [11], (◑) Osada [15], (⊕) Yokoyama [16], (◭) Kay [27], (∗) Critical Point.

Fig. 4. Pressure deviations of $P\rho T$ data from the present model in the vapor phase. (▲) Petty [4], (△) Zubarev [5], (◨) Fischer [6], (◎) Bich [9], (×) Straty [10] , (○) Harrison [11].

Fig. 5. Density deviations of $P\rho T$ data from the present model in the liquid phase. (△) Zubarev [5], (◇) Ta'ani [7], (+) Machado [8], (×) Straty [10] , (○) Harrison [11], (◭) Riembauer [12], (●) Vacek [13], (◆) Xiao [14], (◑) Osada [15], (⊕) Yokoyama [16], (□) Kitajima [3].

Fig. 6. Deviations of measured and calculated vapor-pressure values from the present model. (□) Gibbard [17], (▽) Ambrose [18], (◎) Aim [19], (▲) Cervenkova [20], (◇) Zawiswa [21], (×) de Loos [22], (○) Harrison [11], (+) Lydersen [23], (◑) Osada [15], (⊕) Yokoyama [16], (- - - - - - - -) IUPAC model [2], (————) Eq. (2).

Fig. 7. Deviations of measured and calculated saturated liquid densities from the present model. (+) Yergovich [24], (▲) Hales [25], (◇) Zawiswa [21], (□) Sun [26], (○) Harrison [11], (◑) Osada [15], (⊕) Yokoyama [16], (◭) Kay [27], (- - - - - - - -) IUPAC model [2], (————) Eq. (3).

Fig. 8. Deviations of measured and calculated saturated vapor densities from the present model. (◭) Kay [21], (◇) Zawiswa [21], (□) Sun [26], (○) Harrison [11], (- - - - - - - -) IUPAC model [2], (————) Eq. (4).

Fig. 9. Deviations of the isochoric heat capacity data from the present model. (□) Kitajima

Fig. 10. Deviations of the isobaric heat capacity data from the present model. (+) Stromsoe [28], (◭) Carlson [29], (◎) Counsell [30].

Fig. 11. Deviations of the speed of sound data from the present model. (×) Sun [31], (□) Sun [32], (▽) Boyes [33].

Fig. 12. Calculated isobaric specific heat-capacity values along isobars. (- - - - - - -) IUPAC model [2], (————) the present model.

Fig. 13. Calculated isochoric specific heat-capacity values along isobars. (- - - - - - - -) IUPAC model [2], (————) the present model.

Fig. 14. Calculated speed-of-sound values along isobars using the present model.

Fig. 15. Calculated Joule-Thomson coefficient values along isobars using the present model.

Table I. Sources of Experimental Thermodynamic Property Data for Methanol

First Author [a]	Year	Property	No. of Data	P		ρ		T	
				Range	δP	Range	$\delta\rho$	Range	δT
				(MPa)	(kPa)	(kg · m^{-3})	(kg · m^{-3})	(K)	(mK)
Petty [4]	1955	$P\rho T$	25	0.07 - 1.0	n.a.	1.1 -9.3	0.1	267 -411	n.a.
Zubarev * [5]	1967	$P\rho T$	189	0.4 - 21.8	0.01%	3.9 - 390	0.3	413 - 573	30
Fischer [6]	1972	$P\rho T$	48	0.02 - 0.2	0.01%	0.31 - 1.3		310 - 632	20
Ta'ani [7]	1976	$P\rho T$	194	50 - 800	n.a.	677 - 997	1.4	298 - 623	n.a.
Machado * [8]	1983	$P\rho T$	160	0.5 - 103.8	0.05 %	506 -856	0.1	298 -489	n.a.
Bich [9]	1984	$P\rho T$	19	0.06 - 0.2	0.25 %	0.6 -1.2	n.a.	357 -628	500
Straty * [10]	1986	$P\rho T$	220	2.5 -34.2	n.a.	65 -514	n.a.	378 - 573	n.a.
Harrison * [11]	1989	$P\rho T$	159	0.3 - 40.3	0.01 %	80 -818	n.a.	298 - 533	10
Riembauer * [12]	1990	$P\rho T$	35	0.1 - 300	0.1 %	866 -927	0.2	183 - 213	10
Vacek [13]	1992	$P\rho T$	56	0.4 - 51.5	0.04%	788 - 878	0.11	207 - 297	1
Xiao [14]	1997	$P\rho T$	27	0.1 - 13.5	6	164 -762	0.1	323 - 573	30
Osada * [15]	1999	$P\rho T$	190	0.1 -200	0.1%	651 -884	0.1%	320 - 420	3.0
Yokoyama [16]	2002	$P\rho T$	148	0.1 -200	0.1%	652 -885	0.14%	320 - 420	3.5
Kitajima [3]	2003	$P\rho T$	90	4.3 - 28.4	8	700 -812	0.16	273 - 412	13
Gibbard * [17]	1974	P_S	42	0.009 - 0.01	0.001			288 - 337	2
Ambrose [18]	1975	P_S	11	0.183 - 1.39	n.a.			353 - 453	n.a.
Aim [19]	1980	P_S	17	0.017 - 0.101	0.02			299 - 337	5
Cervenkova [20]	1984	P_S	6	0.04 - 0.097	0.05			316 - 336	10
Zawiswa [21]	1985	P_S	3	0.733 - 2.42	n.a.			398 - 448	n.a.
de Loos [22]	1988	P_S	7	1.38 - 7.73	0.01			422 - 507	50
Harrison * [11]	1989	P_S	9	0.256 - 6.89	n.a.			363 - 511	n.a.
Lyderson [23]	1990	P_S	8	5.96 - 7.98	n.a.			494 - 503	50
Osada * [15]	1999	P_S	14	0.048 - 2.04	0.1			320 - 440	3.0
Yokoyama [16]	2002	P_S	5	0.048 - 1.29	0.1			320 - 420	3.5
Yergovich * [24]	1971	ρ^l	11			800 - 897	0.2	183 - 283	30
Hales [25]	1976	ρ^l	12			620 - 791	0.15	293 - 440	100
Zawiswa [21]	1985	ρ^l	3			605 - 685	n.a.	398 - 448	n.z.
Sun [26]	1988	ρ^l	17			753 - 875	0.02	203 - 333	20
Harrison * [11]	1989	ρ^l	11			436 - 786	n.a.	298 - 503	n.a.
Osada * [15]	1999	ρ^l	6			651 - 765	0.1	320 - 420	3.0
Yokoyama [16]	2002	ρ^l	6			652 - 765	0.14	320 - 420	3.5
Kay [27]	1955	ρ^v	6			33 - 123	n.a.	453 - 503	n.a.
Zawiswa [21]	1985	ρ^v	3			8 - 28	n.a.	398 - 448	n.a.
Harrison [11]	1989	ρ^v	1			125	n.a.	503	n.a.
Stromsoe [28]	1970	C_P	15	0.1	n.a.			347 - 585	n.a.
Carlson * [29]	1971	C_P	17	0.1	n.a.			180 - 325	n.a.
Counsell [30]	1973	C_P	26	0.025 - 0.101	n.a.			330 - 450	n.a.
Kitajima * [3]	2003	C_V	90	4.3 - 28	8			273 - 412	13
Sun * [31]	1988	W	105	0.1 - 276	n.a.			275 - 333	n.a.
Sun * [32]	1990	W	102	0.1 - 276	n.a.			203 - 261	n.a.
Boyes [33]	1992	W	125	0.001 - 0.08	n.a.			280 - 360	n.a.

[a] Data used as input data are denoted by ∗.

Table II. **Summary of Available Critical Parameters for Methanol** [a,b]

First Author	Year	Method [c]	T_c (K)	P_c (MPa)	ρ_c (kg·m^{-3})
Kobe [34]	1953	1	513.17	7.954	272.2
Kay [27]	1955	1	512.60	8.0972	272
Skaates [35]	1964	1	512.68	8.0938	-
Kudchadker [36]	1968	3	512.60	8.0959	272
Zubarev [5]	1969	2	512.67	8.104	275
Zubarev [37]	1973	2	512.61	8.103	-
Ambrose [18]	1980	3	512.60	8.092	272
Craven [38]	1986	3	512.60	8.0972	272
Goodwin [39]	1987	3	512.56	8.09464	269
de Loos [22]	1988	3	512.46	8.06	-
IUPAC [2]	1992	3	512.60 *	8.1035 *	275.56 *

[a] All temperature values in this table were converted to ITS-90.

[b] Critical parameter values used for our modeling are denoted by *.

[c] Method of decision of critical parameter was classified by three ways shown below.

1. Observation of the meniscus.
2. Pressure-volume-temperature relations: $\left(\partial P / \partial \rho\right)_T = 0$
3. Law of rectilinear diameters.

Table III. Coefficients in Eqs. (1) - (3)

i	A_i	B_i	C_i
1	−8.8570247	−1.131507	−0.0770237
2	2.4072447	7.463057	1.686259
3	−2.6452501	−16.52860	−0.5426160
4	−1.5044111	−16.93269	−0.3579365
5		−77.01263	

Table IV. Coefficients in Eq. (5)

i	f_i	g_i
1	2.496674887	-
2	2.900791185	-
3	−62.57135350	-
4	10.99267739	4.119785
5	18.33682995	3.264999
6	−16.36600476	3.769463
7	−6.223234762	2.931493
8	2.803536282	8.225557
9	1.077809894	10.31627
10	0.969656970	0.5324892

Table V. Coefficients in Eq. (6)

i	n_i	d_i	t_i
1	0.12622395×10^{2}	1	0.500
2	-0.83224516×10^{1}	1	0.750
3	-0.14647501×10^{1}	2	0.125
4	-0.12954522×10^{1}	2	1.500
5	0.22417697×10^{0}	3	0.375
6	0.22830533×10^{0}	3	1.750
7	-0.46549039×10^{1}	1	0.000
8	-0.41099957×10^{1}	2	0.500
9	0.70421007×10^{0}	3	1.000
10	0.81617251×10^{-1}	3	3.750
11	-0.37777607×10^{-0}	4	2.000
12	0.19627811×10^{-0}	5	.2.500
13	$0.45571723\times10\text{-}^{2}$	6	0.000
14	-0.11777859×10^{-1}	7	2.500
15	-0.17277890×10^{-4}	8	4.500
16	0.19096856×10^{1}	1	3.000
17	-0.29551319×10^{1}	1	4.000
18	-0.28958480×10^{-0}	2	1.000
19	0.18169967×10^{1}	2	3.000
20	-0.96254996×10^{0}	3	5.000
21	-0.11885503×10^{0}	4	6.000
22	-0.10730710×10^{0}	5	2.500
23	0.15487654×10^{-1}	6	5.000
24	0.66239025×10^{-3}	7	6.000
25	0.15286750×10^{-1}	7	12.000
26	0.31218155×10^{-2}	6	10.000
27	0.14740469×10^{-1}	5	15.000

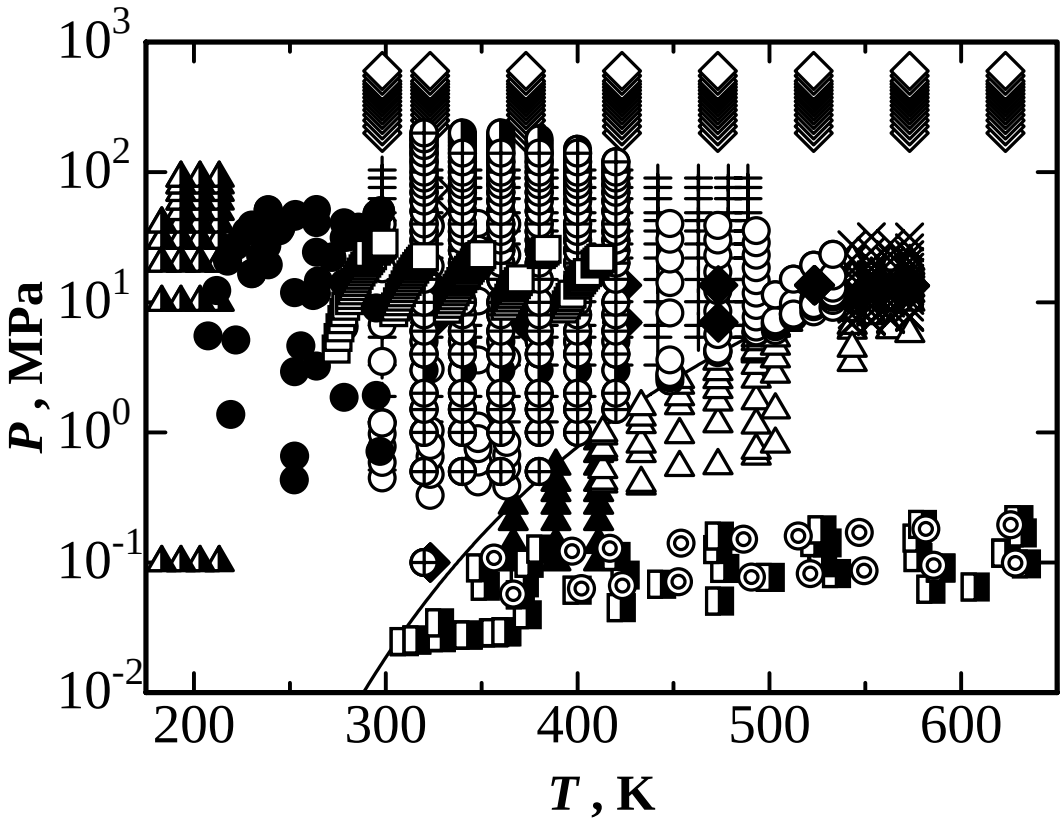

Fig.1

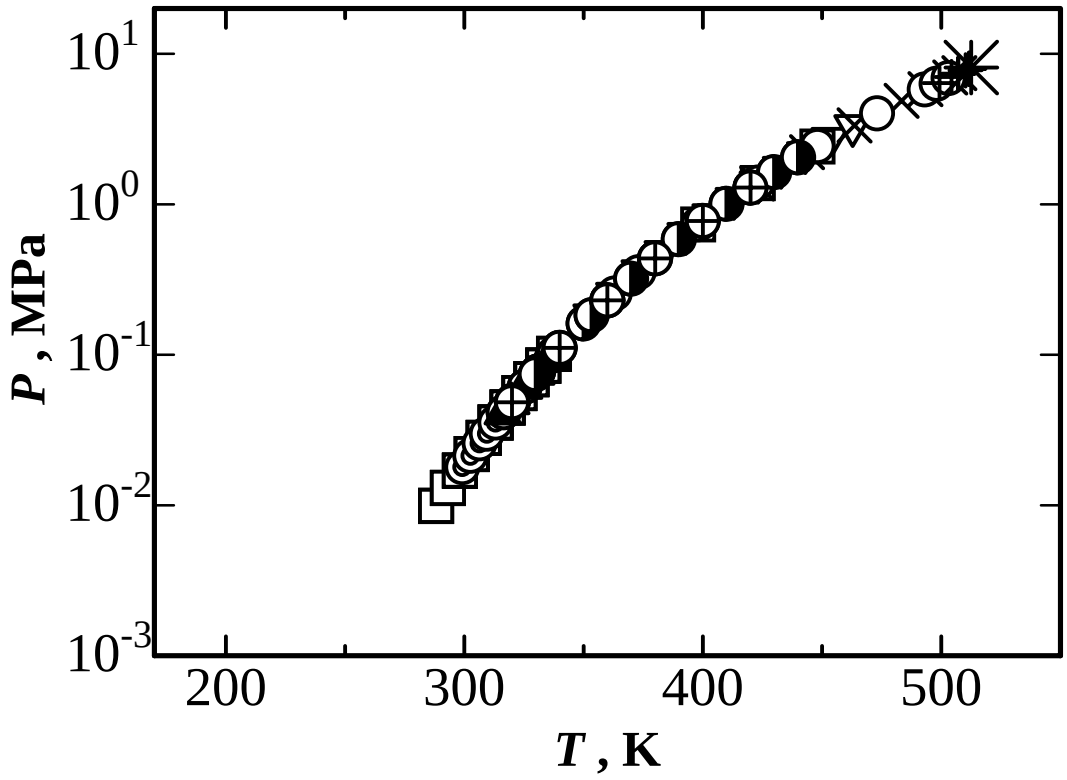

Fig.2.

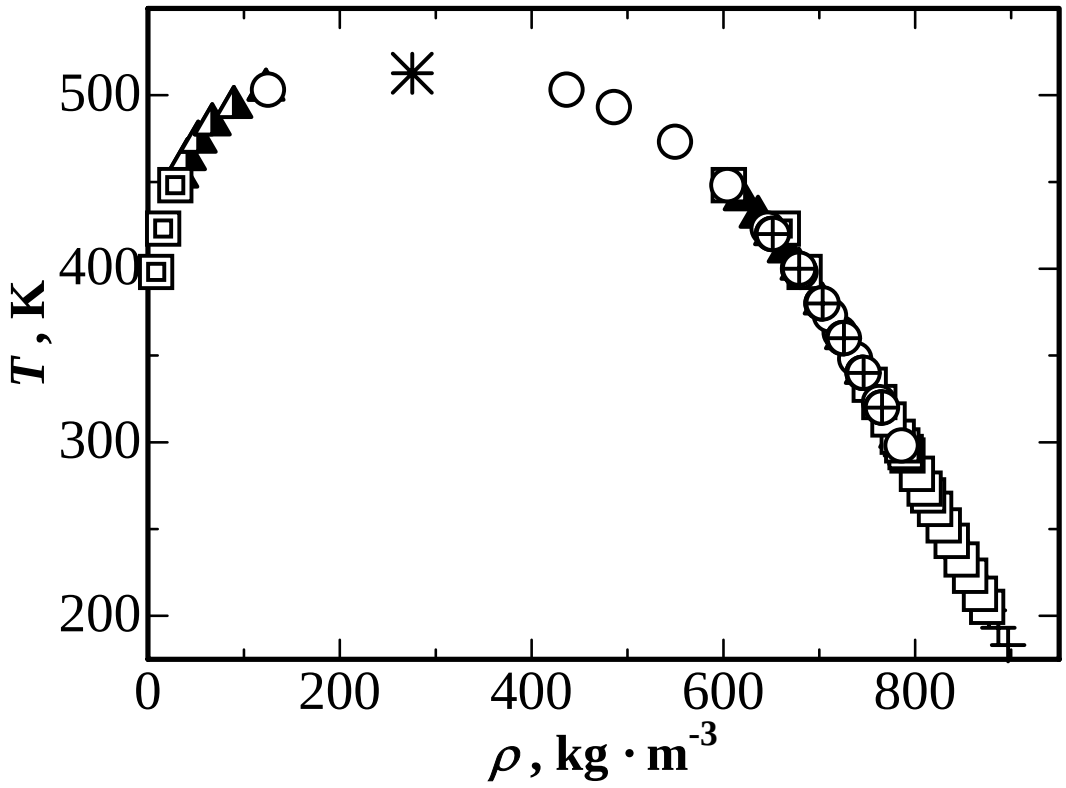

Fig.3

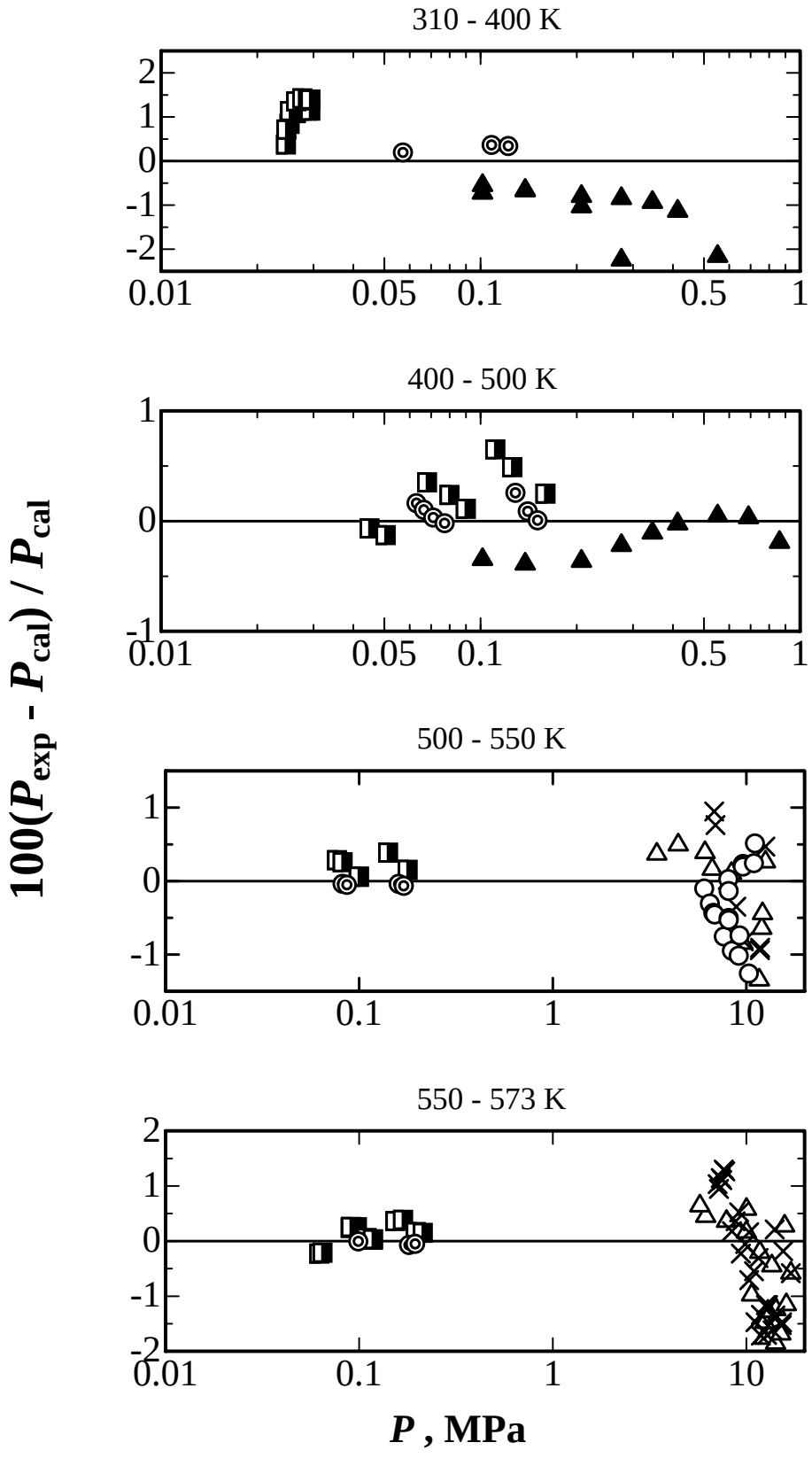

Fig.4

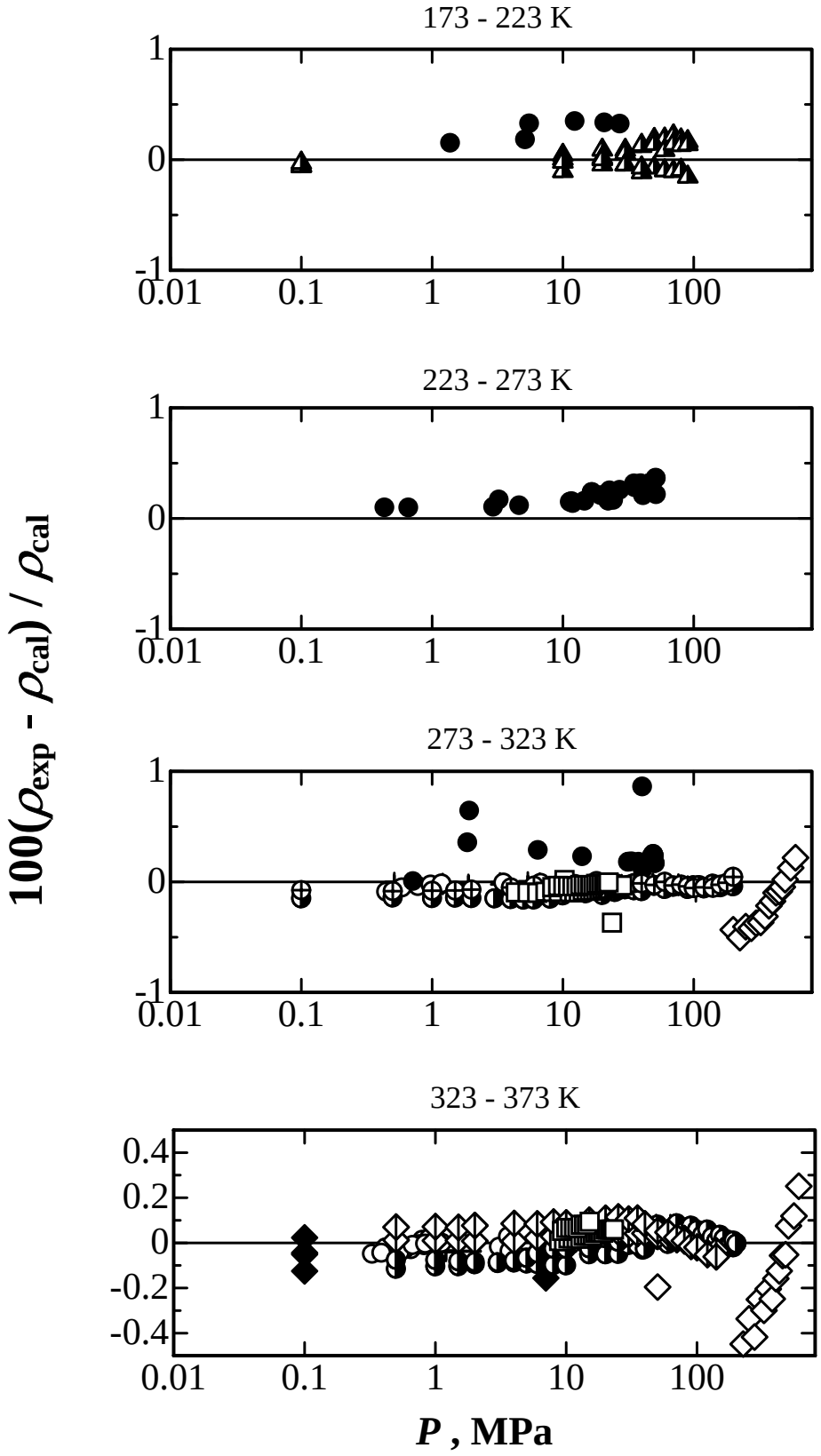
173 - 223 K
223 - 273 K
273 - 323 K
323 - 373 K
100(ρexp - ρcal) / ρcal
P , MPa
1
0
-1
0.4
0.2
-0.2
-0.4
0.01
0.1
1
10
100

Fig.5.

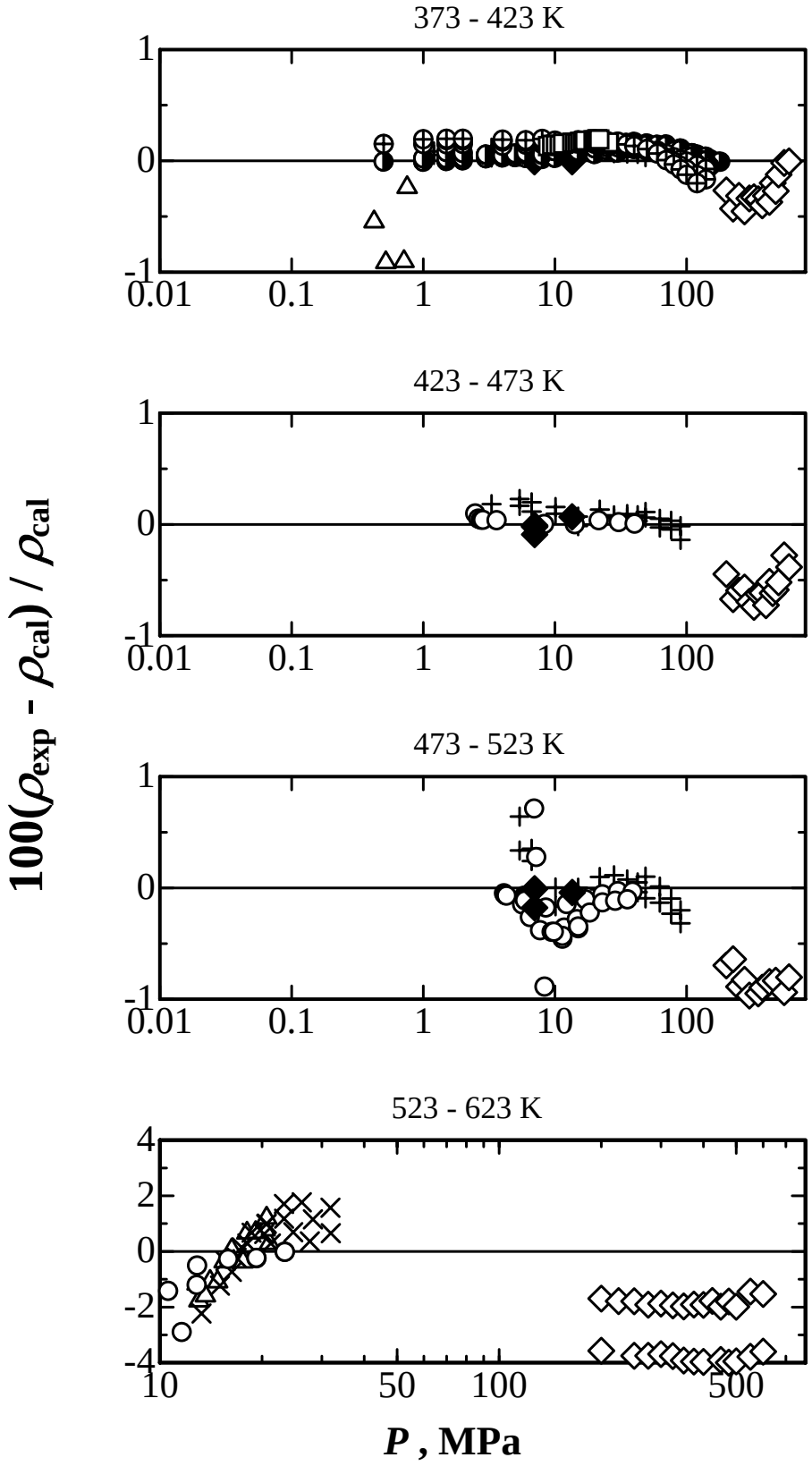

Fig.5 (Continued)

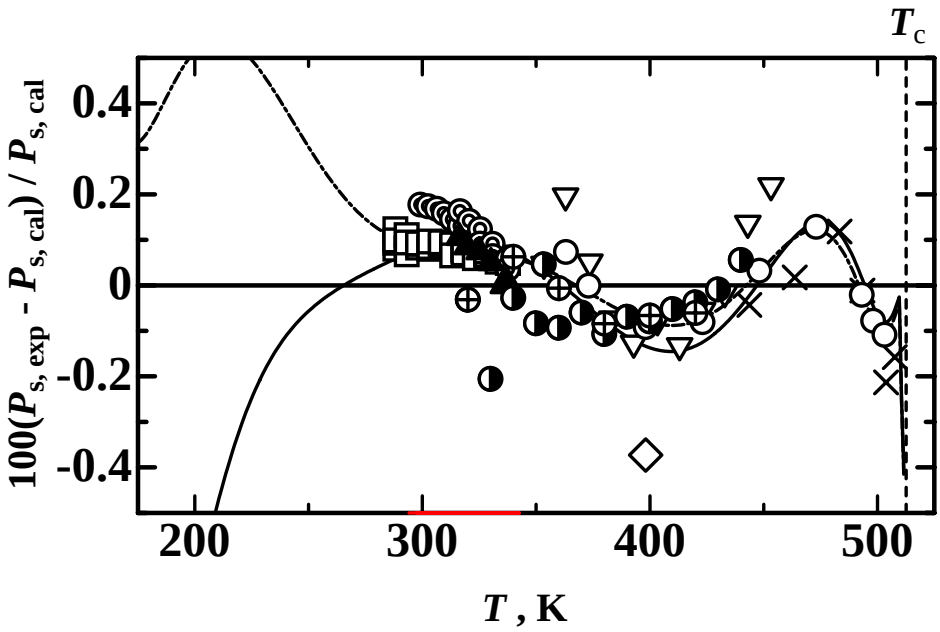

Fig.6

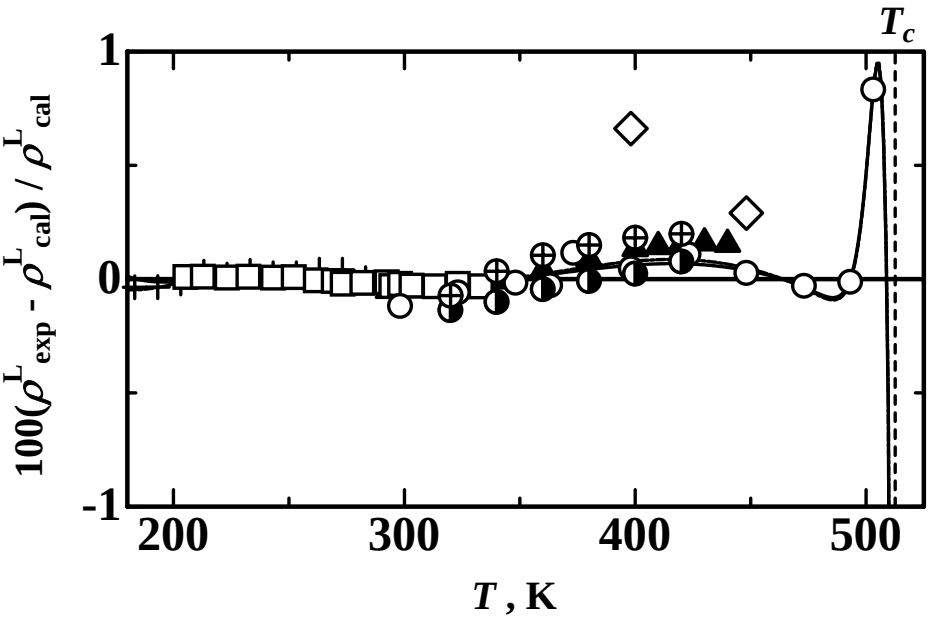

Fig.7

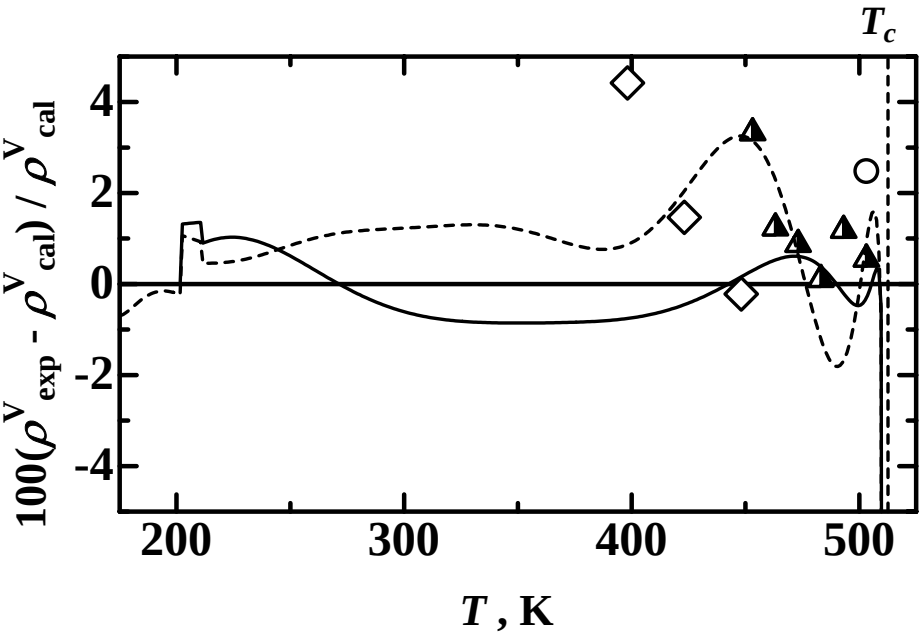

Fig.8

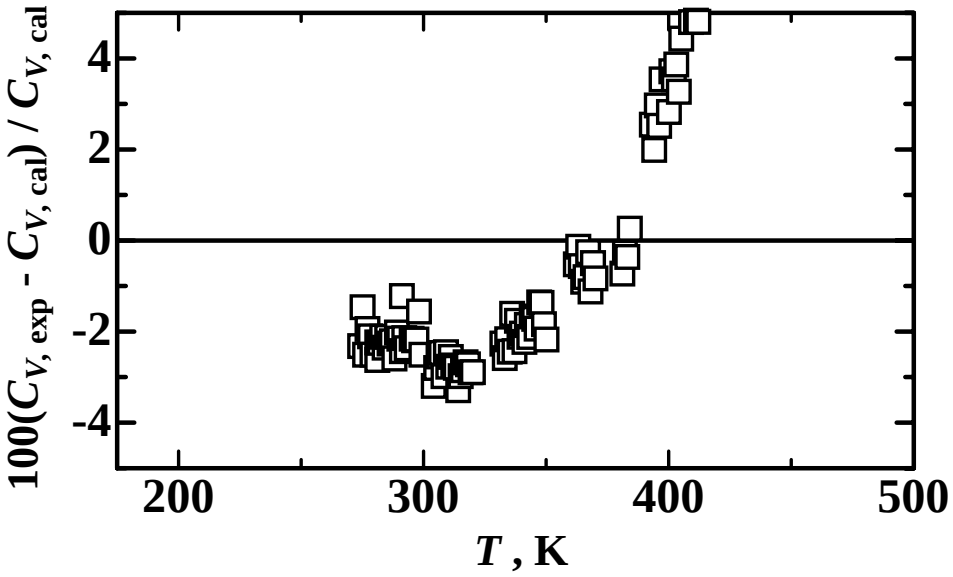

Fig.9

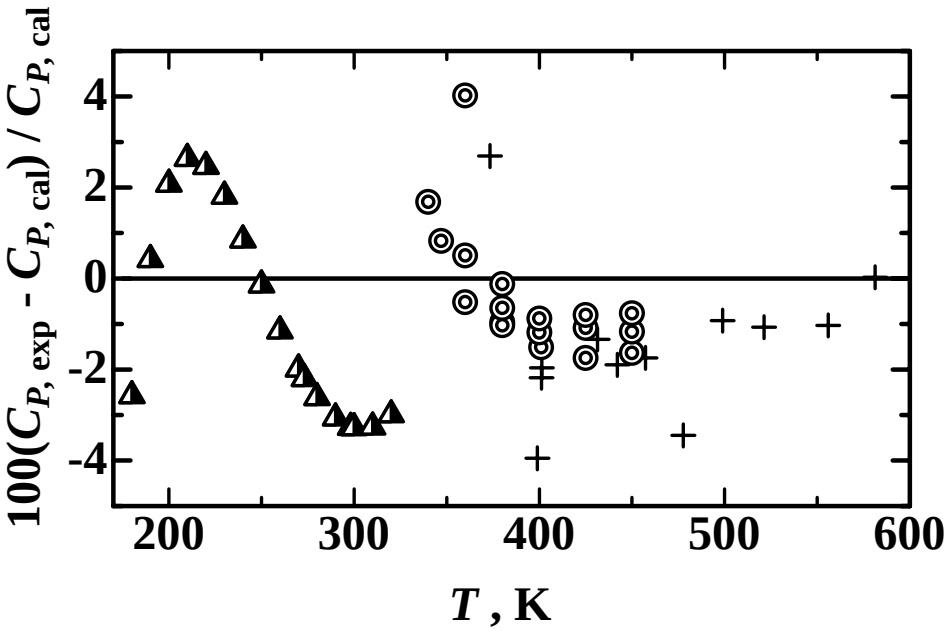

Fig.10

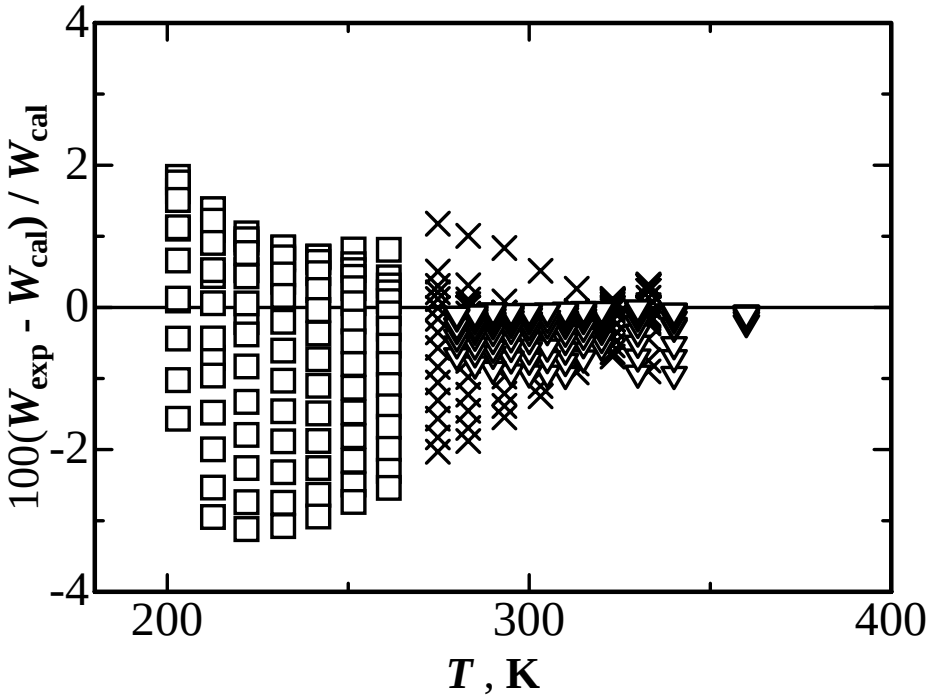

Fig.11

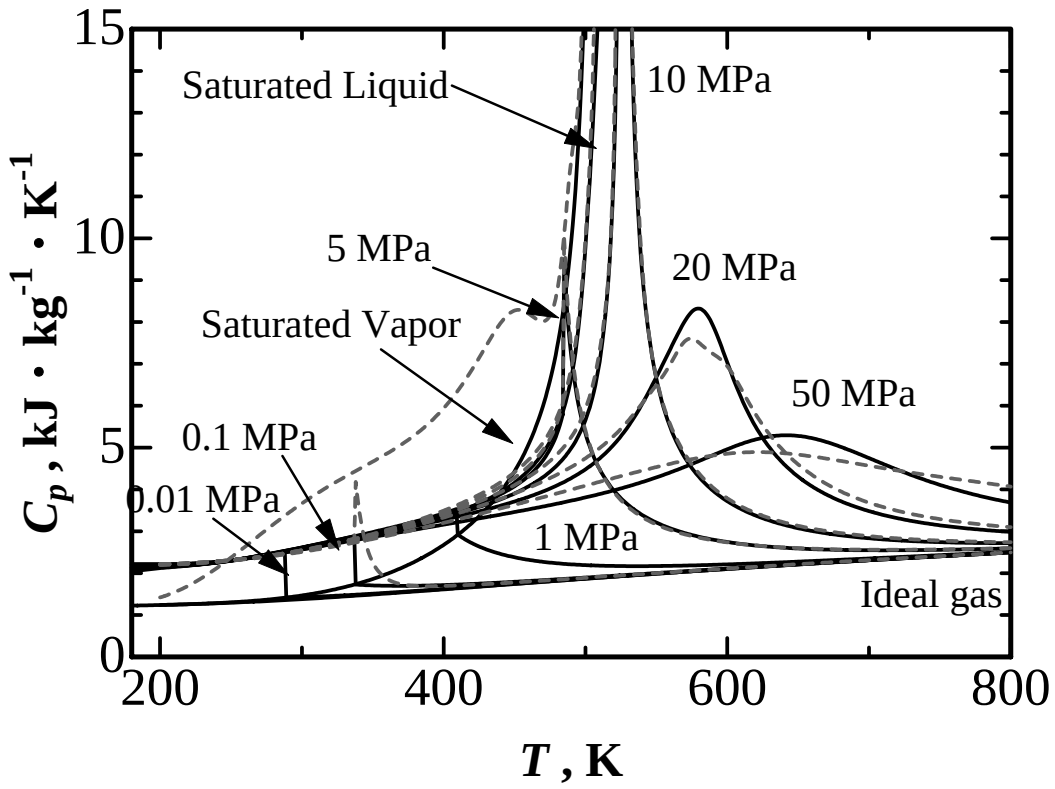
15
10
5
0
200
400
600
800
C_p , kJ • kg^{-1} • K^{-1}
T , K
Saturated Liquid
10 MPa
5 MPa
20 MPa
Saturated Vapor
50 MPa
0.1 MPa
0.01 MPa
1 MPa
Ideal gas

Fig.12

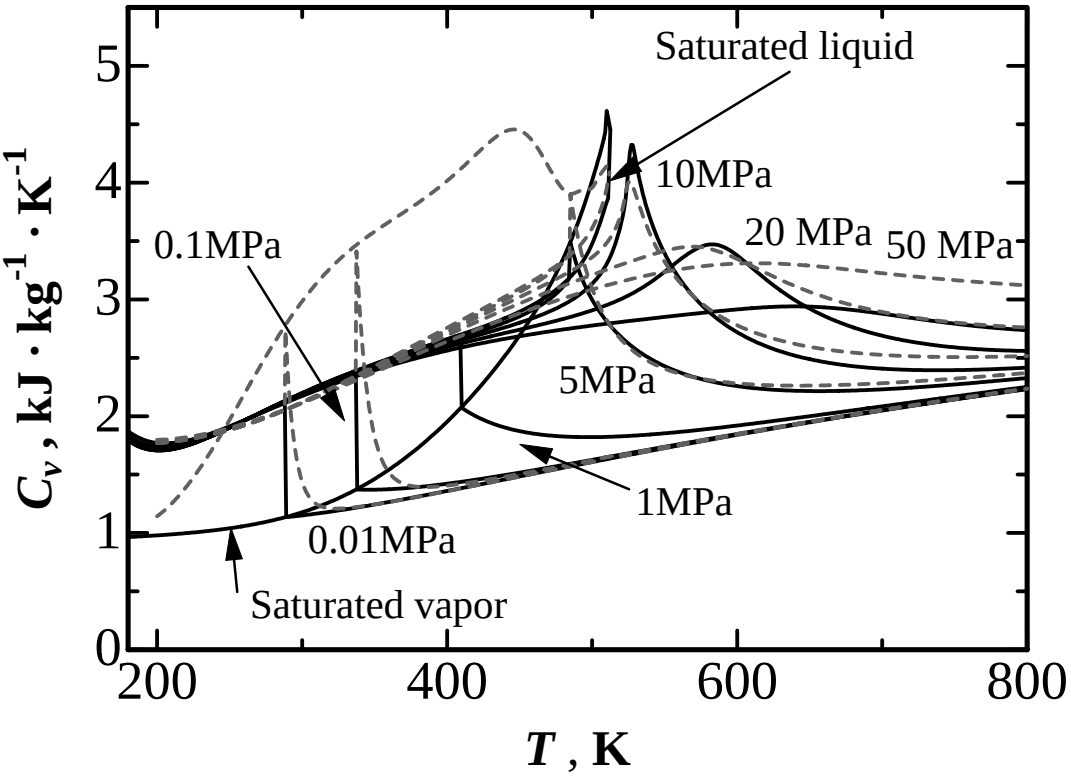
Saturated liquid
10MPa
20 MPa
50 MPa
0.1MPa
5MPa
1MPa
0.01MPa
Saturated vapor
C_v , kJ · kg^{-1} · K^{-1}
T , K
0
1
2
3
4
5
200
400
600
800

Fig.13

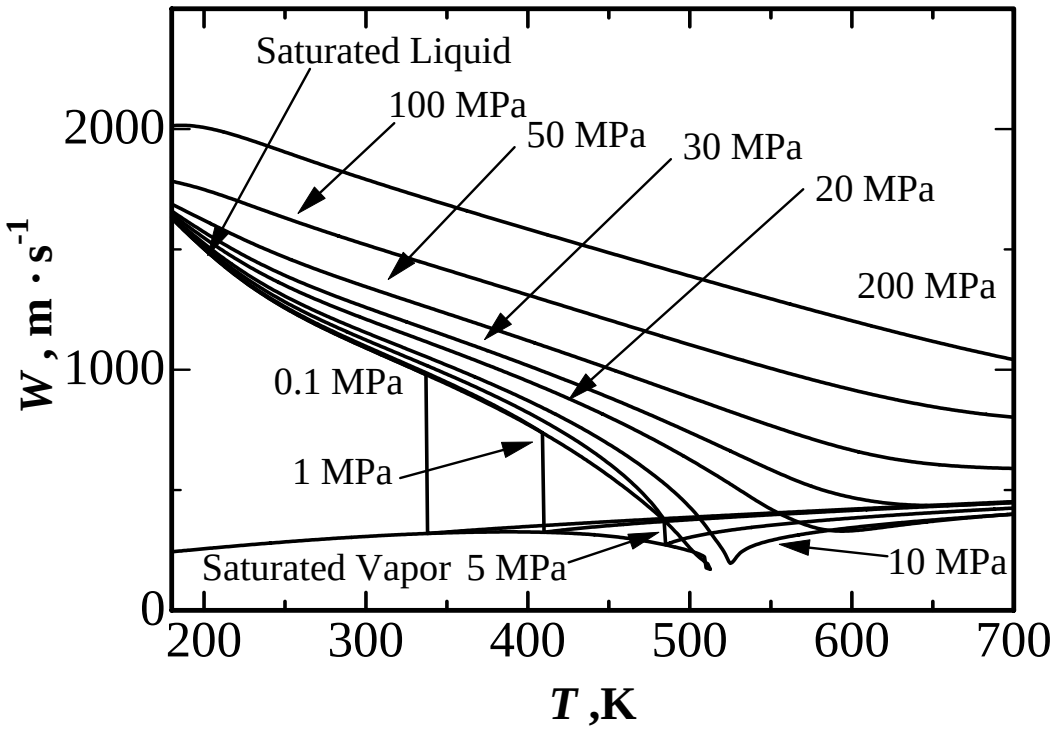
Saturated Liquid
100 MPa
50 MPa
30 MPa
20 MPa
200 MPa
0.1 MPa
1 MPa
Saturated Vapor
5 MPa
10 MPa
2000
1000
0
200
300
400
500
600
700
W , m · s-1
T ,K

Fig.14

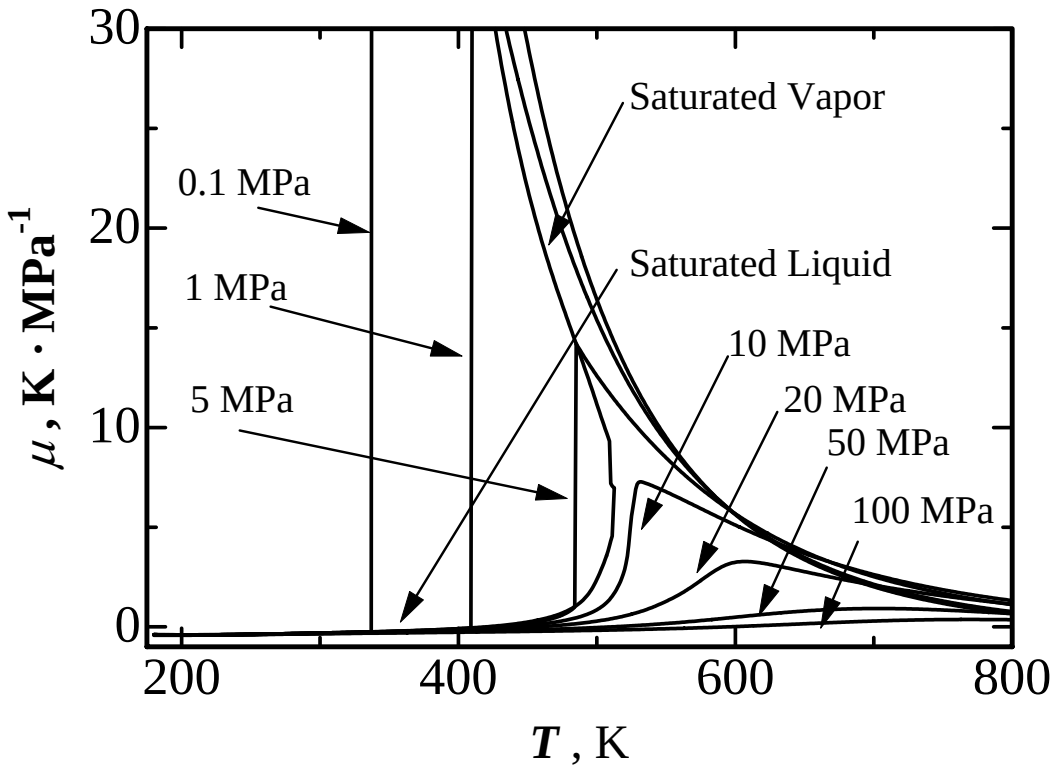
30
20
10
0
200
400
600
800
μ , K · MPa^{-1}
T , K
Saturated Vapor
Saturated Liquid
0.1 MPa
1 MPa
5 MPa
10 MPa
20 MPa
50 MPa
100 MPa

Fig.15